Overexpression of OLC1, Cigarette Smoke, and Human Lung Tumorigenesis

Jingsong Yuan, Jinfang Ma, Hongwei Zheng, Taiping Shi, Wenyue Sun, Qiao Zhang, Dongmei Lin, Kaitai Zhang, Jie He, Yousheng Mao, Xia Gao, Peng Gao, Naijun Han, Guobin Fu, Ting Xiao, Yanning Gao, Dalong Ma, Shujun Cheng

Background Exposure to cigarette smoke is a major risk factor for lung cancer, but how it induces cancer is unclear. The overexpressed in lung cancer 1 (*OLC1*) gene is one of 50 candidate lung cancer genes identified by suppression subtractive hybridization as having higher expression in squamous cell carcinoma (SCC) than normal lung epithelia.

Methods We used immunohistochemistry (IHC) to measure OLC1 protein levels in primary lung cancer samples from 559 patients and used fluorescence in situ hybridization to measure *OLC1* copy number in primary SCC samples from 23 patients. We compared OLC1 protein expression in SCC samples of 371 patients with and without a smoking history using the Pearson χ^2 test. We assayed OLC1 protein levels by immunoblotting in H1299 human lung cancer cells, immortalized human bronchial epithelial cells, and primary cultured normal human bronchial epithelial cells that were treated with cigarette smoke condensate. We assayed tumor formation in athymic mice using NIH3T3 mouse fibroblast cells transfected with OLC1 (eight mice) and analyzed apoptosis and colony formation of H1299 and H520 lung cancer cells transfected with scrambled (negative) or OLC1 small interfering RNAs (siRNAs) (s1).

Results OLC1 protein was overexpressed in 387 of 464 (83.4%) of primary lung cancers, as detected by IHC, and *OLC1* was amplified in 14 of 23 (60%) of SCC samples. OLC1 protein overexpression was more common in SCC patients with a smoking history than those without (77.1% vs 45.8%, $P < .001$). In addition, cigarette smoke condensate increased OLC1 protein levels in H1299 cells, immortalized human bronchial epithelial cells, and primary cultured normal human bronchial epithelial cells. Overexpression of OLC1 induced tumor formation in athymic mice (control vs OLC1, 0% vs 100%). Knockdown of OLC1 increased apoptosis (mean percentage of apoptotic H1299 cells, s1 vs negative: 30.3% vs 6.4%, difference = 23.9%, 95% confidence interval [CI] = 19.1% to 28.5%, $P = .002$; mean percentage of apoptotic H520 cells, s1 vs negative: 21.6% vs 4.9%, difference = 16.7%, 95% CI = 10.6% to 22.8%, $P = .007$) and decreased colony formation (mean no. of colonies of H1299 cells transfected with siRNAs, negative vs s1: 84 vs 4, difference = 80, 95% CI = 71 to 88, $P < .001$; mean no. of colonies of H520 cells transfected with siRNAs, negative vs s1: 103 vs 24, difference = 79, 95% CI = 40 to 116, $P = .005$).

Conclusions *OLC1* is a candidate oncogene in lung cancer whose expression may be regulated by exposure to cigarette smoke.

J Natl Cancer Inst 2008;100:1592–1605

Lung cancer is a leading cause of cancer death worldwide (1), with an estimated 1.2 million new cases diagnosed and 1.1 million deaths every year, according to the World Health Organization. Perhaps more alarming is the fact that the overall survival rate has not substantially improved in the past 20 years (2). To improve the survival of patients with lung cancer, we need to better understand the molecular events involved in lung carcinogenesis. This knowledge is essential to develop novel strategies for early detection and prevention and for individualized therapy. Advances in the study of cancer genetics have shown that expression of many known

Affiliations of authors: Department of Etiology and Carcinogenesis (JY, JM, HZ, WS, KZ, NH, GF, TX, YG, SC), Department of Pathology (DL), and Department of Chest Surgery (JH, YM), Cancer Institute & Hospital, Peking Union Medical College and Chinese Academy of Medical Sciences, Beijing, China; Chinese National Human Genome Center Beijing, Beijing, China (TS, XG, PG, DM); Department of Occupational Health and Toxicology, College of Public Health, Zhengzhou University, Zhengzhou, China (QZ); Human Disease Genomics Center, School of Basic Medical Science, Peking University Health Science Center, Beijing, China (DM).

Correspondence to: Shujun Cheng, Post Graduate; Yanning Gao, MD, PhD; and Dalong Ma, MD, PhD; Department of Chemical Etiology and Carcinogenesis, Cancer Institute & Hospital, Peking Union Medical College and Chinese Academy of Medical Sciences, PO Box 2258, Beijing 100021, People's Republic of China (e-mail: Cheng, chengshj@263.net.cn; Gao, yngao@pubem.cicams.ac.cn; Ma, madl@bjmu.edu.cn).

See "Funding" and "Notes" following "References."

DOI: 10.1093/jnci/djn379

oncogenes, such as MYC, MYB, FOS, KRAS, EGFR, and ERBB2 (3), and several other candidate oncogenes, including SPP1, PTGS2, ADAM9, and STIL (4–7), is frequently associated with lung cancer. Other genes involved in lung cancer have been identified by gene expression profiling of lung cancer using cDNA or oligonucleotide microarrays (8,9), serial analysis of gene expression (10), and suppression subtractive hybridization (SSH) (11).

Most lung cancers are caused by cigarette smoking (12,13), and a key issue for understanding lung carcinogenesis is how cigarette smoke interacts with genes implicated in lung cancer. Cigarette smoke condensate is a complex chemical mixture that contains thousands of different compounds, 100 of which are known carcinogens, cocarcinogens, mutagens, or tumor promoters (14).

We previously used SSH to identify genes with higher expression in squamous cell carcinoma (SCC) than in normal lung epithelium. We then assayed 50 of the identified candidate lung cancer oncogenes for their ability to transform NIH3T3 cells and identified overexpressed in lung cancer 1 (*OLC1*), which was not previously characterized. In this study, we investigated the role of *OLC1* in cigarette smoke-induced human lung carcinogenesis. We measured OLC1 protein levels in primary lung cancer samples and used fluorescence in situ hybridization (FISH) to measure *OLC1* copy number in primary SCC samples. We compared OLC1 protein expression in SCC samples of the patients with and without a smoking history. We assayed OLC1 protein levels in H1299 human lung cancer cells, immortalized human bronchial epithelial cells, and primary cultured normal human bronchial epithelial cells that were treated with cigarette smoke condensate. We assayed the effect of OLC1 overexpression on tumor formation in athymic mice using NIH3T3 mouse fibroblast cells. We also assayed the effect of OLC1 knockdown on apoptosis and on colony formation in H1299 and H520 cells.

CONTEXT AND CAVEATS

Prior knowledge

Exposure to cigarette smoke increases the risk of lung cancer, but the mechanisms involved are unclear.

Study design

Lung cancer and normal lung tissues from patients and cell and animal models of lung cancer were used to examine the effect of overexpression of the gene overexpressed in lung cancer 1 (OLC1) on lung tumorigenesis and how cigarette smoke may be involved.

Contribution

OLC1 protein was overexpressed in the majority of the lung cancer tissues, and the *OLC1* gene was amplified in a majority of lung squamous cell carcinoma samples. High OLC1 protein expression was associated with smoking history and increased expression was observed in cell lines after treatment with cigarette smoke condensate. Knockdown of OLC1 increased apoptosis and decreased colony formation in soft agar.

Implications

OLC1 is a candidate lung cancer oncogene whose expression may be increased by cigarette smoke.

Limitations

The association between OLC1 expression and smoking history was based on few samples from one group of patients. It is unknown how applicable the data generated from these models of lung cancer are to the human disease.

From the Editors

Subjects and Methods

Patients and Tissue Samples

A total of 559 formalin-fixed paraffin-embedded tissue specimens were used to prepare a tissue microarray, which was constructed in the Department of Pathology, Cancer Institute & Hospital, Peking Union Medical College (PUMC) and the Chinese Academy of Medical Sciences (CAMS). The specimens included 346 squamous cell carcinomas (SCCs), 87 adenocarcinomas, 49 small-cell lung cancers (SCLCs), and 77 control samples (normal bronchial epithelia or pulmonary tissues from lung cancer patients). The SCC patients (304 males and 42 females) had a mean age of 66.0 years (range = 31–81 years, SD = 9.4 years), the adenocarcinoma patients (44 males and 43 females) had a mean age of 59.6 years (range = 39–80 years, SD = 10.8 years), the SCLC patients (37 males and 12 females) had a mean age of 57.6 years (range = 28–82 years, SD = 12.5 years), and the control patients (57 males and 20 females) had a mean age of 62.2 years (range = 45–81 years, SD = 9.2 years) at the time of diagnosis. Cancers were clinically staged according to the international tumor-node-metastasis system (15).

An additional 35 primary lung cancer samples from 35 SCC patients and various preneoplastic lesions from the same patient, including dysplasia and/or carcinoma in situ (CIS) on the same slide, were used for immunohistochemical (IHC) staining. These lesions were clinically identified and classified as described previously (16).

For FISH analysis, 23 primary lung cancer samples from 23 SCC patients (20 males and 3 females) were included. These SCC patients had a mean age of 57.9 years (range = 45–70 years, SD = 8.5 years). In the real-time polymerase chain reaction (PCR) experiment, primary lung SCCs and matched normal lung tissues from 22 patients were used. These SCC patients (19 males and 3 females) had a mean age of 60.1 years (range = 45–75 years, SD = 9.2 years).

All patients involved in this study underwent surgical treatment at the Cancer Institute & Hospital, PUMC and CAMS from December 22, 2000, to May 11, 2004. None of the patients had had chemotherapy and/or radiotherapy before surgery. The histopathologic diagnosis was confirmed by two experienced pathologists (D. Lin and H. Zheng). The experimental procedures were reviewed and approved by the ethics committees of the Cancer Institute & Hospital, PUMC and CAMS.

Foci Formation Assay to Screen Candidate Oncogenes in the SSH Library

NIH3T3 (5×10^4 cells per well) were seeded in 24-well plates. The next day, the cells were transfected with the plasmids containing a gene for neomycin resistance and 50 candidate oncogenes from the SSH library we had previously constructed (17) or empty vector control. Each plasmid was transfected in triplicate wells. Geneticin (Invitrogen, Carlsbad, CA, 800 μg/mL) was added 24 hours later. Foci were counted 2 weeks after the cells reached confluence.

FISH Analysis to Determine OLC1 Gene Copy Number

FISH analysis was performed according to standard protocols as previously described (18). After surgical resection, primary SCC samples from 23 patients as described above were collected by aspiration using a 23-gauge needle, and thin-layer slides of cells were prepared using a ThinPrep 2000 processor (Cytyc, Boxborough, MA) according to the manufacturer's instructions. A bacterial artificial chromosome (BAC) clone containing *OLC1* was obtained from the BACPAC Resources Center (BPRC, Oakland, CA), and labeled directly with cy3-dUTP using Bioprime DNA labeling kit (Invitrogen). A chromosome 16 centromere-specific probe was labeled directly with fluorescein-12-dUTP (Roche, Basel, Switzerland) and hybridized to the slides simultaneously with the BAC-OLC1 probe. Chromosomes were counterstained with 4′,6-diamidino-2-phenylindole. Tumor samples showing sufficient hybridization efficiency (>90% nuclei with signals) were evaluated; 100 intact nuclei per slide were scored for number of signals. Tumor signals were scored as gains when at least 20% of cells showed three or more signals of the BAC-*OLC1* probe (19). Only cells with a malignant cytological appearance (especially large nuclei) were scored. Small round lymphocyte-like cells and cells with overlapping or damaged nuclei were disregarded. The signals of the centromeric probes were used to control for adequate hybridization and to exclude artifacts. Two probe signals were counted as one if they were very close to each other (<0.5 μm), to avoid misinterpretation due to sister chromatids of cells in S or G2/M phase (20).

Real-Time PCR to Evaluate the Relative Genomic Copy Number of OLC1

The relative genomic copy number of *OLC1* was evaluated in primary lung SCCs and matched normal lung tissues from 22 patients (described above) by real-time PCR on the ABI 7300 Sequence Detection System (Applied Biosystems, Foster, CA) as previously described (21). Primers for *OLC1* were 5′-TTAGGTG AGTGTGGCATCC-3′ (forward) and 5′-CCCACTTCCA CTATCCTTCC-3′ (reverse) (GenBank accession number AK057902). Thermal cycling consisted of an initial denaturing step at 95°C for 10 minutes, then 40 cycles of 95°C for 5 seconds, 57°C for 31 seconds, and 72°C for 45 seconds. β-*actin* was used as the input reference with the primers 5′-CCTGTACGCCAA CACAGTGC-3′ (forward) and 5′-ATACTCCTGCTTGCT GATCC-3′ (reverse) (GenBank accession number NM_001101). Results are shown as relative copy number (*OLC1*/*Actin*), and the samples with higher than 1.5-fold change were considered as having positive amplification.

Gene Cloning and Plasmid Construction

We cloned the *OLC1* gene using gene prediction, expressed sequence tag (EST) assembly, and rapid amplification of cDNA ends. Two independent EST clones in the lung cancer SSH library that we previously constructed for SCC (17) of genes that had increased expression in SCC were included in the same entry (UniGene: Hs.232194, with the gene symbol: KIAA0174). The mRNA sequence AK057902 encodes the full-length OLC1 protein because it has an in-frame stop codon at the 5′-end, upstream of the putative ATG start codon, and a polyadenylation sequence at the 3′-end (data not shown). Using reverse transcription (RT)–PCR, we cloned the full-length open reading frame into pcDNA3.1/mycHis(–) B (Invitrogen). We sequenced the vectors using an ABI PRISM 3730 DNA Analyzer (Applied Biosystems). The primers used for RT–PCR cloning were 5′-TAGGAGGAACAGCACAGCATG-3′ (forward) and 5′-AGTTGCCTGGTTTAAGAGACCTATG-3′ (reverse). Similarly, the full-length open reading frame of OLC1 was also cloned into pcDNA3.1/Hygro+ (Invitrogen), which contained hygromycin as a selection marker.

Antibody Preparation and IHC Staining to Evaluate OLC1 Protein Expression

The entire open reading frame of OLC1 was inserted into pGEX-4T-1 (GE Healthcare, Munich, Germany) and expressed as recombinant glutathione-S-transferase–OLC1, which was purified and used to produce a polyclonal rabbit antibody against OLC1 by Sanying Biotechnology, Inc (Wuhan, China). The tissue microarray was constructed as previously described (22). IHC staining was performed on 5-μm sections cut from the tissue microarray block (n = 559) or other slides (n = 35) as described previously (4) using a 1:100 dilution of the primary polyclonal rabbit anti-OLC1 antibody. The slides were blindly labeled and scored by two independent observers (D. Lin and H. Zheng) using previously described criteria (4). Briefly, the percentage of the cells with cytoplasmic labeling was recorded from two areas of each specimen, and the labeling intensity was estimated as 1+, 2+, or 3+ for weak, moderate, or strong staining. The IHC results were categorized as follows: samples without any labeling, with 1+ labeling in less than 25% cells, or with 2+ labeling in less than 10% cells were defined as negative, and all the remaining samples were defined as positive.

Cell Lines, Cell Culture, and Transfections

Mouse fibroblast NIH3T3, human cervical adenocarcinoma HeLa, and the human lung cancer cell lines A549, H520, H2170, and H1299 were obtained from the American Type Culture Collection (Manassas, VA). The immortalized human bronchial epithelial cell lines MBE, YBE, Tr, and C45 were established and maintained by our laboratory (23,24). A549, H520, H2170, and H1299 cells were maintained in Dulbecco's modified Eagle's medium (DMEM, HyClone, Logan, UT) containing 10% fetal bovine serum (FBS, HyClone). NIH3T3 cells were maintained in DMEM with 10% bovine calf serum (HyClone). Plasmid transfection was performed using Lipofectamine 2000 (Invitrogen) according to the manufacturer's instructions. For selection of stable clones, OLC1 and the constitutively active mutant of H-Ras (H-Ras^{Val12}) in pcDNA3.1/mycHis(–)B, or the empty vector were transfected into NIH3T3 cells and selected with geneticin (Invitrogen) at 800 μg/mL; in addition, OLC1 in pcDNA3.1/Hygro+ or the empty vector were transfected into MBE cells and selected with hygromycin (Invitrogen) at 500 μg/mL for 6 weeks by modified limiting dilution. This method generated three NIH3T3 clones (OLC1-C1, OLC1-C2, and OLC1-C3) and six MBE clones (C1–C6). Because C4 had the highest level of OLC1 protein expression, it was designated as MBE-OLC1 and was used in subsequent experiments.

RNA Interference to Knock Down OLC1 Expression

For experiments using small interfering RNAs (siRNAs) targeted to OLC1, two Silencer predesigned siRNA duplexes were selected,

synthesized, and purified using polyacrylamide gel electrophoresis (PAGE) by Ambion, Inc (Austin, TX). The siRNA sequences were as follows: s1, 5′-GGAAGGAGAUUGCUGACUAtt-3′ (sense); s2, 5′-GGAGAUUGCUGACUAUCUGtt-3′ (sense). Scrambled sequence siRNA (Ambion, Inc) was used as a negative control. The OLC1 siRNAs or scrambled siRNA were transfected into H1299 and H520 cells using Lipofectamine 2000 (Invitrogen) according to the manufacturer's instructions for siRNA transfection. Mock-transfected cells were also prepared as negative controls.

Flow Cytometry Assay for Apoptosis

Apoptotic H1299 and H520 cells that had been mock transfected or transfected with s1, s2, or scrambled siRNA were stained with fluorescein isothiocyanate–conjugated annexin V and propidium iodide (PI) as described previously (25). Cells were analyzed on a FACSCalibur flow cytometer (Becton Dickinson, Franklin Lakes, NJ), with excitation using a 488-nm argon ion laser. PI staining was used to distinguish necrotic and late apoptotic events (annexin V−, PI+; annexin V+, PI+) from early apoptotic events (annexin V+, PI−). The experiments were repeated twice.

Preparation of Cigarette Smoke Condensate to Test Its Effects on OLC1 Expression in a Lung Cancer Cell Line, an Immortalized Human Bronchial Epithelial Cell Line, and Primary Cultured Normal Human Bronchial Epithelial Cells

The cigarette smoke condensate was prepared from the most popular type of cigarette in China (Honghe, 15 mg tar, 1.2 mg nicotine) as described previously (26). Briefly, a "water-pipe" smoking device was designed and operated to allow a stream of smoke to flow into a tubular shaped trap, which was maintained at room temperature, and then into a 2-L flask submerged in liquid nitrogen. The amount of smoke obtained was determined by the weight increase of the flask. Cigarette smoke condensate was prepared by dissolving the collected smoke particulates in dimethyl sulfoxide (DMSO) at 20 mg/mL. The condensate was divided into small vials and stored at −80°C. On the day of the experiment, the cigarette smoke condensate solution was diluted in serum-free culture media to the desired concentration and used for cell treatment. Briefly, cigarette smoke condensate at 1 μg/mL was added to treat MBE, PBE, and H1299 cells for 0, 0.5, 2, 12, 24, 36, and 48 hours; in the experiment with different concentrations, MBE cells were treated with cigarette smoke condensate at 0, 0.5, 1, and 2 μg/mL for 24 hours. Control cells were treated with medium containing an equivalent amount of DMSO.

Immunoblotting

Immunoblotting analysis was performed on lysates of A549, H520, H2170, H1299, MBE-37, YBE-11, Tr, and C45 cells; MBE, H1299, and primary cultured normal human bronchial epithelial (PBE) cells that had been treated with cigarette smoke condensate; parental NIH3T3 and NIH3T3 cells that had been transfected with empty vector or OLC1 (three clones); parental MBE cells and MBE cells that had been transfected with empty vector or OLC1 (six clones); and H1299 and H520 cells that had been mock transfected or transfected with OLC1 siRNAs (s1 or s2) or scrambled siRNA. Cell lysates were prepared by incubation of cells with RIPA buffer supplemented with protease inhibitor (Pierce, Rockford, IL) and phosphatase inhibitor (Sigma-Aldrich, St Louis, MO). Proteins (30–60 μg) were separated by 10% sodium dodecyl sulfate–PAGE and electrophoretically transferred to Immobilon-P membranes (Millipore, Bedford, MA). The membranes were incubated for 30 minutes in phosphate-buffered saline (PBS; 0.1 M sodium phosphate and 0.15 M sodium chloride, pH 7.4) containing 0.1% Tween 20 and 5% nonfat milk to block nonspecific binding and were then incubated for 2 hours at room temperature with rabbit polyclonal anti-OLC1 (1:1000), rabbit polyclonal anti-poly ADP ribose polymerase (1:1000; Cell Signaling, Danvers, MA), and mouse monoclonal anti–β-actin (1:5000, Sigma-Aldrich) antibodies. The membranes were washed three times for 10 minutes in PBS with 0.1% Tween 20 and then incubated for 1 hour with a goat anti-rabbit or goat anti-mouse horseradish peroxidase–conjugated secondary antibody (1:1000; Santa Cruz Biotechnology, Santa Cruz, CA). The membranes were washed three times for 10 minutes in PBS with 0.1% Tween 20, and the antibody reactivity was visualized with the SuperSignal West Pico Chemiluminescent Substrate (Pierce). All experiments were repeated three times.

Cell Proliferation Assay

Cell growth rate was measured by the tetrazolium salt 3-(4,5-dimethylthiazol-2-yl)-2,5-diphenyltetrazolium bromide (MTT) assay using the CellTiter 96 Non-Radioactive Cell Proliferation Assay Kit (Promega, Madison, WI). Briefly, NIH3T3 clones (2×10^3 cells) and H1299 and H520 cells (1×10^3) that had been mock transfected or transfected with OLC1 siRNAs and scrambled siRNA were seeded per well in 96-well plates in replicates of six, and the assay was performed at 24-hour intervals (0–120 and 0–96 hours, respectively) according to the manufacturer's protocol with a few modifications. The growth rates of MBE-OLC1 and MBE-vector cells were assayed by counting daily for 8 days. Briefly, MBE-OLC1 and MBE-vector cells (6.5×10^4 cells) were seeded into six-well plates in triplicate wells. The cells were dislodged by incubation with trypsin–EDTA and counted each day with a hemocytometer. The trypan blue dye (Sigma-Aldrich) exclusion method was used to identify viable cells. All experiments were repeated three times.

Colony Formation Assay

H1299 and H520 cells were harvested 48 hours after transfection (mock or with OLC1 siRNAs or scrambled siRNA) by incubation in trypsin–EDTA (Invitrogen) and seeded at a density of 500 cells per well in triplicate on six-well plates. Ten days later, the plates were washed with PBS, and the cells were fixed in cold methanol and stained with 0.5% crystal violet. Colonies larger than 1 mm in diameter were counted. All experiments were repeated three times.

Soft Agar Assay

The soft agar assay was performed as described previously (23). Briefly, parental NIH3T3 cells and stable NIH3T3 clones transfected with empty vector, H-Ras^{Val12}, and OLC1 plasmids (5×10^3 cells each) were placed in 1.5 mL per well of DMEM with 0.35% agarose and 10% FBS and overlaid onto 1.5 mL per well of DMEM with 0.5% agar and 10% FBS in six-well plates. After 2 weeks, colonies larger than 200 μm in diameter were counted. The assay was repeated three times in triplicate for each cell clone.

Tumorigenicity in Nude Mice

Female BALB/c athymic mice (nu/nu, 4 weeks old, n = 18) were purchased from the Animal Center, PUMC and CAMS (Beijing, China), housed under aseptic conditions, and cared for in accordance with the guidelines of the Animal Center, PUMC and CAMS. Mice were injected subcutaneously with parental NIH3T3 cells (n = 5 mice), NIH3T3 cells transfected with empty vector (n = 5 mice), and an NIH3T3 OLC1-overexpressing stable clone (n = 8 mice) (5×10^6 cells per mouse). Tumor size was measured every 3 days, and tumor volume (V) was estimated from the length (L) and width (W) of the tumors using the formula: $V = (\pi/6) \times [(L + W)/2]$ (27). All mouse experiments were approved by the Animal Center, PUMC and CAMS.

Statistical Methods

The association between IHC staining of OLC1 and other clinical parameters (including histological grade and patient stage, age, and sex) was assessed using the chi-square test. We used the Pearson chi-square test to determine the relationship between OLC1 protein expression in the tissue samples of primary lung SCC and the smoking history of 371 patients from the Cancer Institute & Hospital, PUMC and CAMS. The SCC patients with a smoking history smoked a mean of 38.6 pack-years (range = 10–90 pack-years). We used generalized estimating equation (GEE) methods (28) to determine the statistical significance of the differences of OLC1 expression between the normal tissues and lung cancer tissues from the same group of lung cancer patients; we also used GEE methods to perform pairwise comparisons of OLC1 expression in various preneoplastic and neoplastic lesions from patients with primary lung SCCs. The Student t test was used for all other comparisons. All statistical tests were two-sided. Differences with P values less than .05 were considered statistically significant. The GEE analysis was performed using SAS version 9.1 (SAS Institute, Cary, NC). All other calculations were performed using the Statistical Package for the Social Sciences (SPSS), version 11.5 (SPSS Inc, Chicago, IL).

Results

Identification of OLC1 From SSH Libraries

Through our previously constructed SSH libraries of genes whose expression was increased or decreased in SCC (17), we identified 50 candidate genes. To identify genes in the SSH library for which increased expression had inherent oncogenic potential, we transfected each of them into NIH3T3 cells. After 2 weeks of growth after the cells reached confluence, cells overexpressing one gene (known as rlcrt-000196 in the library) had formed obvious foci, indicating cell transformation (Figure 1, A). We designated rlcrt-000196 as OLC1 for "overexpressed in lung cancer 1." The SSH library of genes whose expression was increased in SCC contained two independent EST clones for OLC1 (Figure 1, B).

OLC1 (also known as KIAA0174, accession number AK057902) spans 33.47 kb on human chromosome 16q22.2 and encodes a predicted 364-amino acid protein (approximately 40 kDa). The protein sequence contains a DUF292 domain that is uncharacterized, has amino acid sequences that are evolutionarily conserved across species (from bacteria to human) at its amino terminus (Figure 1, C and D), and has a proline-rich region (residues 220–278) near the carboxyl terminus.

OLC1 Protein Overexpression and Gene Amplification in Lung Cancers

Expression levels of OLC1 were measured in lung cancer cell lines by immunoblotting and in primary lung cancer tissues by immunohistochemical staining. On immunoblots, OLC1 was recognized at a molecular weight of about 40 kDa (Supplementary Figure 1, available online). OLC1 protein levels were higher in lung cancer cell lines than in immortalized normal human bronchial epithelial cell lines (Figure 2, A). Immunofluorescence staining of OLC1 and green fluorescent protein-OLC1 fusion protein were localized in the cytoplasm (Supplementary Figures 2 and 3, available online). We performed control experiments using antibody pre-absorbed with OLC1 antigen and with nonimmune globulin; the OLC1 antibody gave a specific staining pattern (Supplementary Figure 4, C, available online). We also performed an OLC1 knockdown experiment. When OLC1 was depleted using OLC1 siRNA in H520 cells, the fluorescence signal was obviously weaker than that in the cells with control siRNA (Supplementary Figure 4, A and B, available online).

We analyzed OLC1 expression by IHC in a tissue microarray containing 559 paraffin-embedded tissue samples. Staining was successful in 537 of 559 (96.1%) of the tissue samples. OLC1 protein was overexpressed in 387 of 464 (83.4%) of primary lung cancers, including 263 of 336 (78.3%) primary lung SCCs, 79 of 83 (95.2%) ADCs, and 45 of 45 (100%) SCLCs separately, but in only 17 of 73 (23.3%) of the normal lung tissues adjacent to the tumors (Figure 2, B; Table 1; $P < .001$). No associations between IHC staining of OLC1 and other clinical parameters (histological grade or patient stage, age, or sex) were observed, as assessed using the chi-square test.

To determine whether the OLC1 gene was amplified in lung cancers, we used FISH to measure *OLC1* copy number in primary lung SCCs. We observed OLC1 gene amplification in 14 of 23 (60%) of the primary tumors (Figure 2, C). Amplification of *OLC1* was also confirmed by real-time PCR in 10 of 22 (45%) patients with primary lung SCCs and matched normal lung tissues (Figure 2, D).

OLC1 Overexpression and Cigarette Smoking in Lung Tumorigenesis

Cigarette smoke is the major cause of upper aerodigestive tract cancers. To determine whether OLC1 overexpression is associated with the smoking history of patients with lung cancer, we analyzed OLC1 protein expression in samples of primary lung SCCs from 371 patients (from the Cancer Institute & Hospital, PUMC and CAMS) with the patients' smoking history. OLC1 protein was overexpressed in a larger proportion of samples from patients who had smoked than from those who had not (77.1% vs 45.8%, $P < .001$; Figure 3, C). Consistent with the clinical observation, cigarette smoke condensate treatment induced expression of OLC1 protein in a lung cancer cell line, an immortalized human

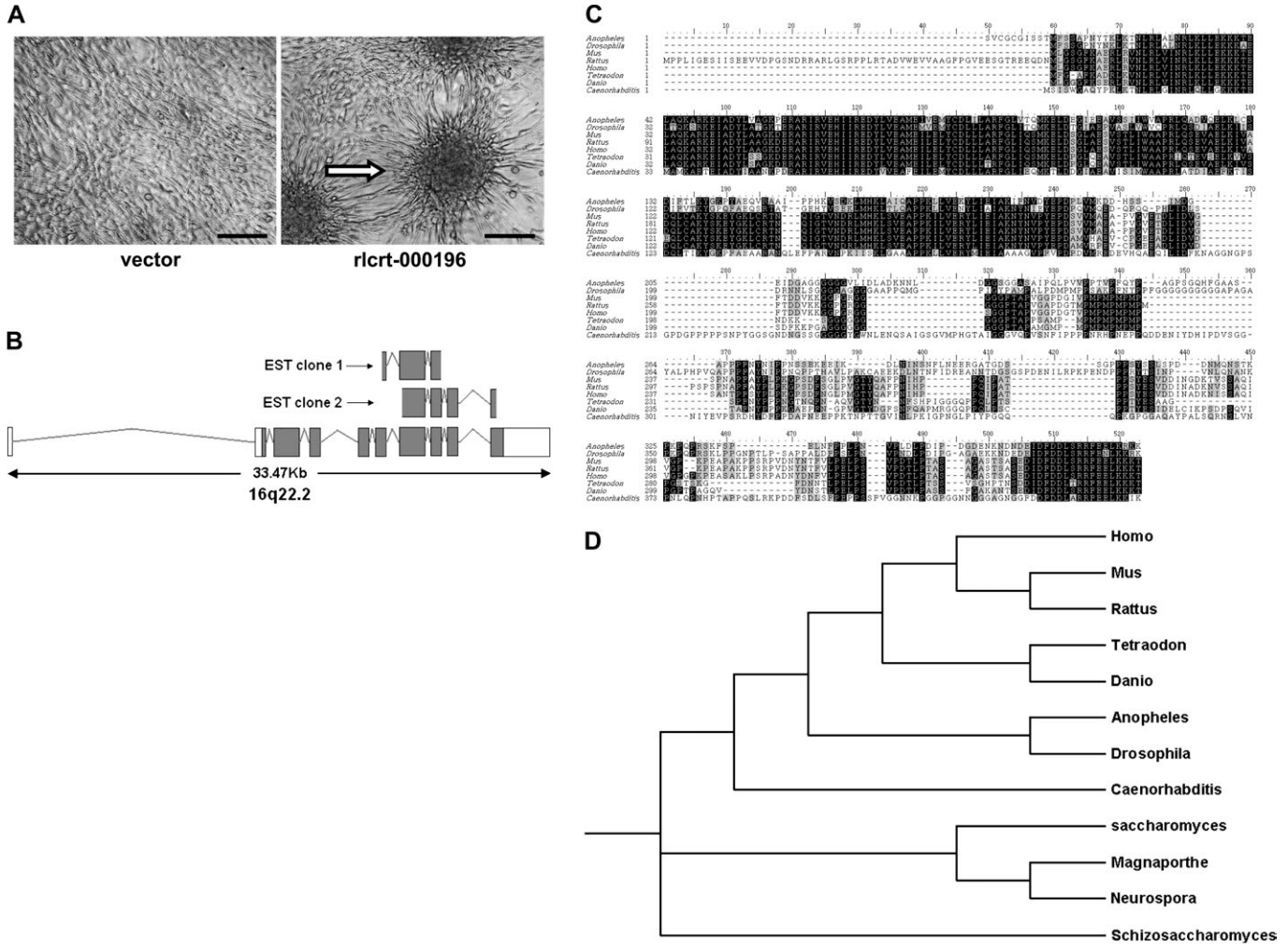

Figure 1. Identification of overexpressed in lung cancer 1 (*OLC1*) from suppression subtractive hybridization (SSH) libraries through phenotype-based screening. **A**) Phenotype-based screening in NIH3T3 mouse fibroblast cells. The foci formation assay was performed with Geneticin selection for 3 weeks after transfection. Foci formation in rlcrt-000196–transfected cells is indicated with an **arrow**. Scale bar = 100 μm. **B**) Genomic alignment of two independent expressed sequence tag (EST) clones to OLC1 in the SSH library. **C**) Comparison of OLC1 amino acid sequences from different species. Black and gray shading indicates identical and **conserved** residues, respectively. **D**) Phylogenetic trees for OLC1. The protein sequences were obtained by conceptual translation of GenBank DNA entries from each species corresponding to the following accession numbers. *Homo sapiens*: P53990; *Mus musculus*: NP_082294; *Rattus norvegicus*: XP_226448; *Anopheles gambiae*: XP_315909; *Drosophila melanogaster*: NP_648058; *Caenorhabditis elegans*: NP_506170; *Tetraodon nigroviridis*: CAF92099; *Danio rerio*: NP_997750; *Saccharomyces cerevisiae*: P53843; *Schizosaccharomyces pombe*: NP_588331; *Magnaporthe grisea*: XP_363839; *Neurospora crassa*: XP_328697. The alignment was generated by using ClustalX version 1.83 (41), and **phylogenetic** tree analysis was performed by TreeView X version 0.4 which can be accessed from http://darwin.zoology.gla.ac.uk/~rpage/treeviewx/.

bronchial epithelial cell line, and in primary cultured normal human bronchial epithelial cells (Figure 3, D).

To determine whether OLC1 overexpression occurs early in lung carcinogenesis, we compared OLC1 protein expression in various preneoplastic and neoplastic lesions from patients with primary lung SCCs (Figure 3, A). The frequencies of OLC1 antibody-positive lesions from normal bronchial epithelia, hyperplasia, dysplasia/CIS, and primary lung SCC were 9 of 32 (28.1%), 6 of 21 (28.6%), 13 of 16 (81.3%), and 34 of 35 (97.1%), respectively (Figure 3, B).

Oncogenic Properties of OLC1

To assess the oncogenic potential of OLC1, we established NIH3T3 clones that stably express OLC1 (Figure 4, A). These clones grew faster than the vector-transfected control cells, as assayed by MTT assay (Figure 4, B). H-Ras^{Val12}–transformed NIH3T3 cells were used as a positive control. (Mean OD [570–630 nm] of OLC1-C1 vs the vector-transfected control cells [Vector] at 120 hours: 1.13 vs 0.75, difference = 0.38, 95% confidence interval [CI] = 0.33 to 0.43, $P < .001$; OLC1-C2 vs Vector: 1.06 vs 0.75, difference = 0.32, 95% CI = 0.24 to 0.39, $P < .001$; OLC1-C3 vs Vector: 1.06 vs 0.75, difference = 0.32, 95% CI = 0.28 to 0.35, $P < .001$). Two weeks after seeding on soft agar, each of the three clones expressing OLC1 and the H-Ras^{Val12}–transfected NIH3T3 cells formed colonies, but the parental NIH3T3 cells and the cells transfected with empty vector did not (Figure 4, C).

To test the tumorigenicity of OLC1 in vivo, parental NIH3T3 cells, NIH3T3 cells that were transfected with empty vector, and

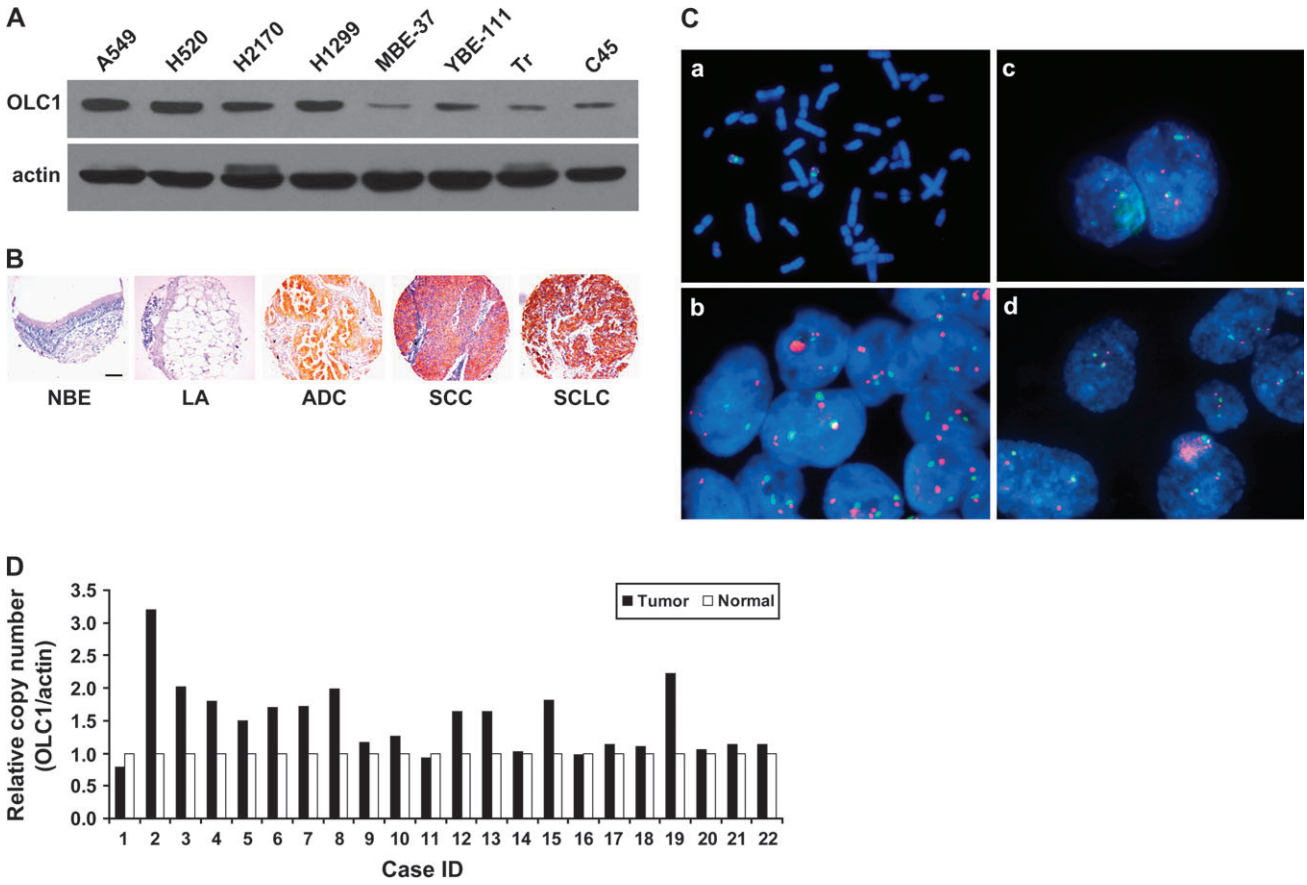

Figure 2. Overexpression and amplification of overexpressed in lung cancer 1 (OLC1) in lung cancer tissues and cell lines. **A**) Immunoblot of OLC1 in lung cancer cell lines (A549, H520, H2170, and H1299) and immortalized bronchial epithelial cell lines (MBE, YBE, Tr, and C45) using a rabbit polyclonal anti-OLC1 antibody. Blots were probed with mouse monoclonal anti–β-actin antibody as a control for loading and transfer. A representative blot from three independent experiments is shown. **B**) Representative examples of tissue microarray–based immunohistochemical staining of OLC1 in human lung cancer and normal lung tissues using a rabbit polyclonal anti-OLC1 antibody in (A). Scale bar = 100 μm. Lung adenocarcinoma (ADC), squamous cell carcinoma (SCC), and small-cell lung cancer (SCLC) showed positive staining, but samples of normal bronchial epithelia (NBE) and lung alveolus (LA) appeared negative. **C**) Amplification of *OLC1* detected by fluorescence in situ hybridization. a, metaphase spread showing that the OLC1 bacterial artificial chromosome (BAC) maps to 16q22; b, the H2170 cell line has 4-6 OLC1–hybridizing loci (**red**); c, this lung SCC has five copies of OLC1; d, this lung SCC has two copies each of OLC1 and chromosome 16 centromere (**green**). **D**) Pairwise comparison of *OLC1* genomic copy numbers in lung SCC and matched normal lung tissues from 22 patients. Results are shown as relative copy number (*OLC1*/Actin) from three replicates. β-actin was used as the input reference.

NIH3T3 clone OLC1-C1 cells were injected into nude mice. Fibrosarcomas formed in all eight mice that were injected with OLC1-expressing NIH3T3 cells, but not in mice (n = 5 per group) that were injected with the parental or empty vector–transfected cells (Figure 4, D and E).

To determine the effect of OLC1 overexpression on the tumorigenicity of a cell line derived from normal bronchial epithelia, we generated OLC1-overexpressing MBE cells (Figure 4, F). MBE is an immortalized human bronchial epithelial cell line with low levels of OLC1 expression. Compared with

Table 1. Immunohistochemical staining for OLC1 in the samples from tissue microarray*

Tissue samples	No. of samples	No. of positive samples (%)	*P*†
Normal lung tissues	73	17 (23.3)	
Primary lung SCC	336	263 (78.3)	<.001‡
Primary lung ADC	83	79 (95.2)	<.001§
Primary SCLC	45	45 (100)	N/A

* OLC1 = overexpressed in lung cancer 1; SCC = squamous cell carcinoma; ADC = adenocarcinoma; SCLC = small-cell lung cancer. N/A = not applicable with generalized estimating equation (GEE) method due to the 100% frequency of OLC1 expression in primary SCLC. Notably, the morphologically normal tissues (including 49 samples of bronchial epithelia and 24 of alveolus) were collected from the same group of lung cancer patients.

† *P* values (two-sided) were calculated using GEE analysis with 1 degree of freedom.

‡ Primary lung SCC vs normal lung tissues.

§ Primary lung ADC vs normal lung tissues.

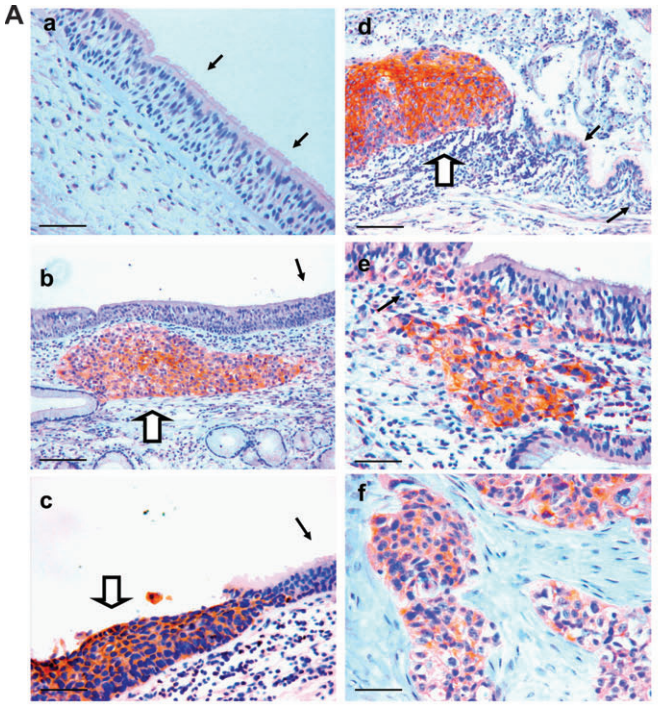

C

Smoking history of lung SCC patients	OLC1 expression [n (%)] in cancer tissues -	+	OR (95% CI)	P
without smoking history	45 (54.2%)	38 (45.8%)	3.9 (2.4 to 6.6)	<.001*
with smoking history	66 (22.9%)	222 (77.1%)		

Smoking history status: with a mean of 38.6 pack-years (range = 10 to 90 pack-years)

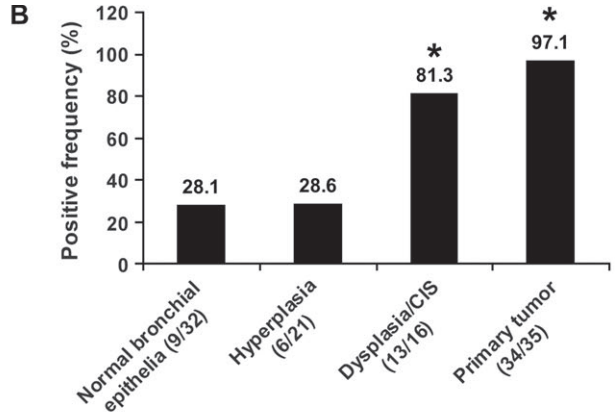

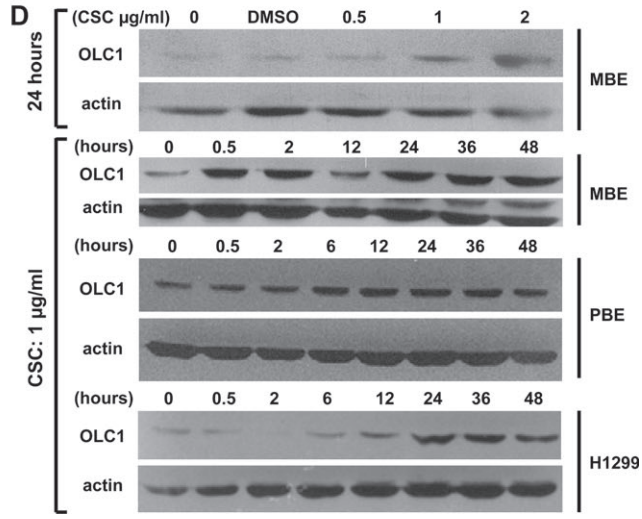

Figure 3. The association of overexpressed in lung cancer 1 (OLC1) overexpression with cigarette smoking and lung tumorigenesis. **A**) Representative examples of immunohistochemical (IHC) staining of OLC1 in lung squamous cell carcinoma (SCC) tissue samples from 35 lung SCC patients with various preneoplastic or neoplastic lesions using a rabbit polyclonal anti-OLC1 antibody. a, normal bronchial epithelia indicated by **black arrows**, negative; b, hyperplasia (**black arrow**, negative) and a primary SCC (**open arrow**, positive); c, severe dysplasia (**open arrow**, positive) and the nearby normal bronchial epithelia (**black arrow**, negative); d, carcinoma in situ (CIS, **open arrow**, positive) and the nearby normal bronchial epithelia (**black arrows**, negative); e, SCC nest, scattered cancer cells in the basal layer (**open arrow**, positive), and the adjacent normal epithelia (**black arrow**, negative); f, primary SCC of the lung, positive. Scale bars in a, c, e, and f represent 50 µm and those in b and d represent 100 µm. **B**) Results of IHC staining for OLC1, performed as described in (A), in lung SCC tissue samples from 35 lung SCC patients with various preneoplastic or neoplastic lesions. *Primary tumor vs normal bronchial epithelia: $P < .001$; primary tumor vs hyperplasia: $P < .001$; dysplasia/CIS vs hyperplasia: $P < .001$; dysplasia/CIS vs normal bronchial epithelia: $P < .001$. All P values were two-sided and calculated using generalized estimating equation (GEE) analysis, with 1 degree of freedom. **C**) OLC1 protein overexpression as detected by IHC in the paraffin-embedded tissue samples of primary lung SCCs from 371 patients and smoking history in these lung SCC patients. *$P < .001$ (two-sided), calculated using the Pearson chi-square test with 1 degree of freedom. **D**) Cigarette smoke condensate (CSC) treatment and OLC1 overexpression in MBE, H1299, and primary cultured normal human bronchial epithelial (PBE) cells. Immunoblot analysis of OLC1 expression using the OLC1 antibody in (A). A total of 60 µg of total protein was loaded from MBE and PBE cells, and 10 µg of total protein was loaded from H1299 cells. Blots were probed with mouse monoclonal anti–β-actin antibody as a control for protein loading and transfer. One representative blot from three independent experiments is shown.

MBE-vector control cells, MBE-OLC1 cells grew faster in culture (mean number of cells [$\times 10^4$] of MBE-OLC1 vs MBE-vector cells on day 7: 103.3 vs 70.2, difference = 33.1, 95% CI = 24.2 to 42.0, $P < .001$) and formed more colonies (mean no. of colonies of MBE-OLC1 vs MBE-vector cells: 136 vs 60, difference = 76, 95% CI = 70 to 82, $P < .001$) (Figure 4, G and H). MBE-OLC1 cells also had an accelerated G1/S phase transition compared with MBE-vector control cells (mean percentage of cells in G1 phase, MBE-OLC1 vs MBE-vector: 10.7% vs 26.5%, difference = 15.8%, 95% CI = 18.2% to 13.4%, $P < .001$; mean percentage of cells in S phase, MBE-OLC1 vs MBE-vector: 55.0% vs 39.1%, difference = 15.9%, 95% CI = 9.9% to 21.9%, $P = .002$) (Figure 4, I). However, we did not observe any difference between MBE-OLC1 and MBE-vector cells in terms of growth in soft agar, and no tumors were found in nude mice injected with MBE-OLC1 cells (data not shown).

To examine the role of OLC1 overexpression in cancer cells, we used RNA interference technology to silence OLC1 expression in lung cancer cell lines. We transfected H520 and H1299 cells with two siRNA duplexes (OLC1-s1 and OLC1-s2). Both siRNA sequences were located in the third exon of the OLC1 gene (Figure 5, A). In both H520 and H1299 lung cancer

cell lines, the siRNAs efficiently knocked down the expression of OLC1 at both the mRNA and protein levels (Figure 5, B). Seventy-two hours after transfection, higher percentages of cells that were transfected with OLC1 siRNAs underwent apoptosis than negative control cells (mean percentage of apoptotic H1299 cells, s1 vs negative: 30.3% vs 6.4%, difference = 23.9%, 95% CI = 19.1% to 28.5%, $P = .002$; s2 vs negative: 12.5% vs 6.4%, difference = 6.1%, 95% CI = 1.0% to 11.1%, $P = .035$; mean percentage of apoptotic H520 cells, s1 vs negative: 21.6% vs 4.9%, difference = 16.7%, 95% CI = 10.6% to 22.8%, $P = .007$; s2 vs negative: 18.2% vs 4.9%, difference = 13.3%, 95% CI = 9.5% to 17.0%, $P = .004$.) (Figure 5, C and D). The fact that the cells underwent apoptosis was confirmed by detecting cleavage of PARP (Figure 5, G). When the growth rate was assessed by MTT assay, cells transfected with OLC1 siRNAs grew more slowly than the negative control cells (mean OD [570–630 nm] of H1299 cells at 96 hours after transfection with siRNAs, negative vs s1: 1.03 vs 0.07, difference = 0.96, 95% CI = 0.83 to 1.10, $P < .001$; negative vs s2: 1.03 vs 0.41, difference = 0.62, 95% CI = 0.47 to 0.77, $P < .001$. Mean OD [570–630 nm] of H520 cells at 96 hours after transfection with siRNAs, negative vs s1: 0.66 vs 0.21, difference = 0.44, 95% CI = 0.39 to 0.50, $P < .001$; negative vs s2: 0.66 vs 0.29, difference = 0.37, 95% CI = 0.31 to 0.42, $P < .001$. Figure 5, E). In addition, we observed a statistically significant inhibition of colony formation in both H1299 and H520 cells after OLC1 siRNA transfection (mean no. of colonies of H1299 cells transfected with siRNAs, negative vs s1: 84 vs 4, difference = 80, 95% CI = 71 to 88, $P < .001$; negative vs s2: 84 vs 37, difference = 47, 95% CI = 35 to 57, $P < .001$. Mean no. of colonies of H520 cells transfected with siRNAs, negative vs s1: 103 vs 24, difference = 79, 95% CI = 40 to 116, $P = .005$; negative vs s2: 103 vs 24, difference = 79, 95% CI = 39 to 119, $P = .005$. Figure 5, F).

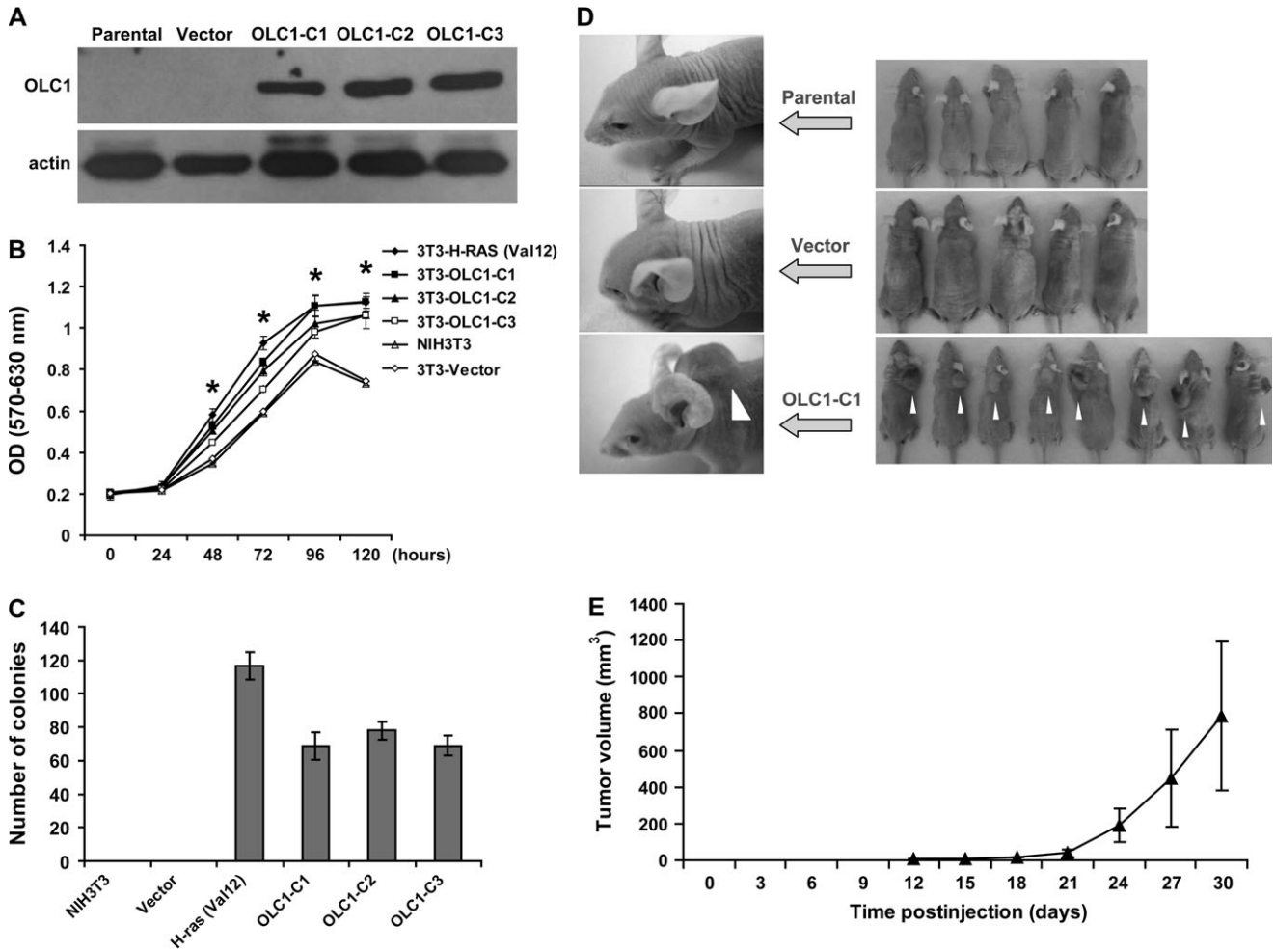

Figure 4. Effect of overexpressed in lung cancer 1 (OLC1) overexpression on NIH3T3 and MBE cells. **A**) Immunoblot of untransfected NIH3T3 cells (Parental), NIH3T3 cells transfected with empty vector (Vector), and NIH3T3 clones (OLC1-C1 through C3) transfected with OLC1 DNA, using a rabbit polyclonal anti-OLC1 antibody. Blots were probed with monoclonal mouse anti–β-actin antibody to control for protein loading and transfer. One representative of three independent experiments is shown. **B**) The tetrazolium salt 3-(4,5-dimethylthiazol-2-yl)-2,5-diphenyltetrazolium bromide proliferation assay of NIH3T3 cell clones in (A). H-Ras^{Val12}–transformed NIH3T3 cells were used as a positive control. Means and 95% confidence intervals (CIs, **error bars**) are shown. **Error bars** represent 95% CIs for three independent experiments performed in triplicate. *OLC1-C1, C2, C3, or H-Ras^{Val12}–transformed NIH3T3 cells vs Vector, $P < .001$. **C**) Numbers of colonies in the soft agar assay from the three OLC1 NIH3T3 cell clones (C1–C3), the NIH3T3 parental line, and vector control cells. Colonies larger than

(continued)

Figure 4 (continued).

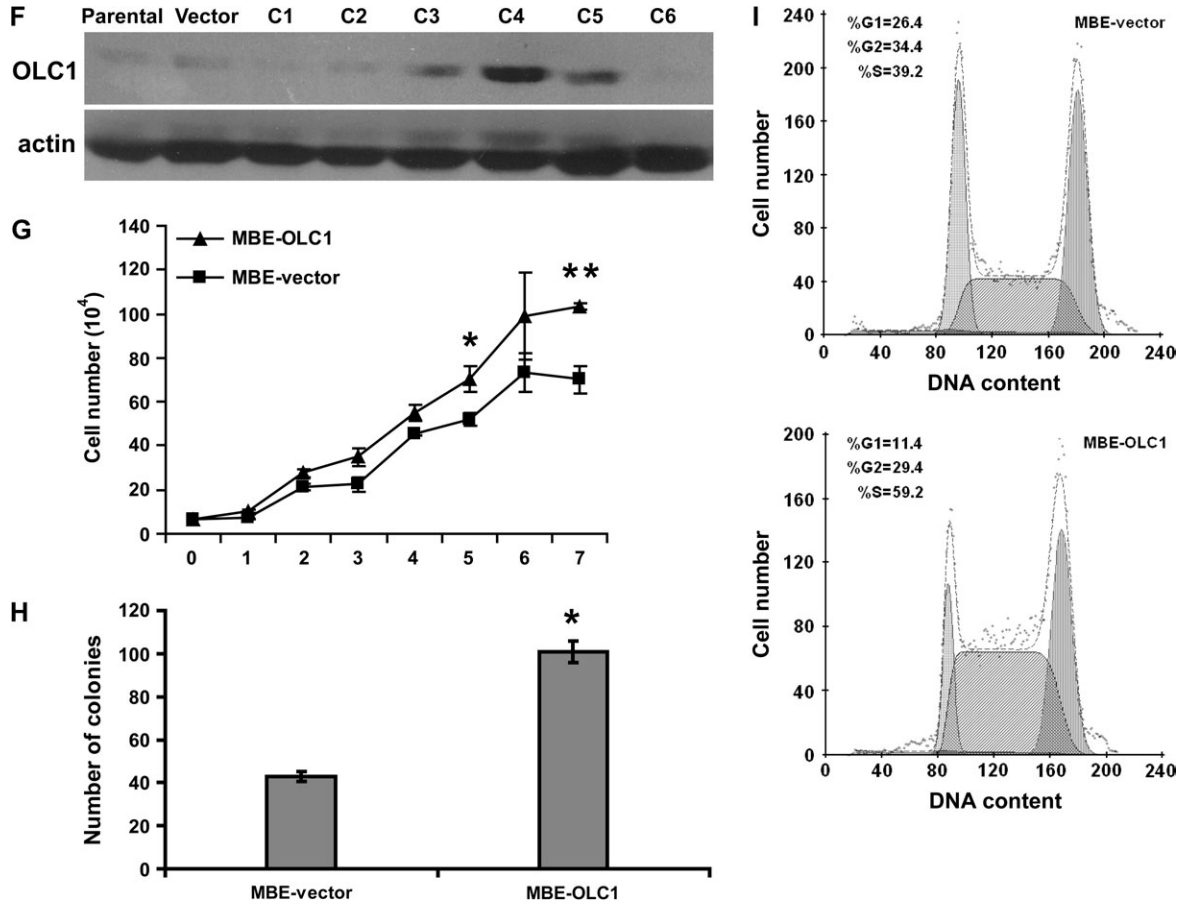

200 μm in diameter were counted. Means and 95% CIs (**error bars**) are shown from three independent experiments performed in triplicate. **D**, **E**) Tumors observed in nude mice inoculated NIH3T3 parental, vector, or OLC1-C1 (**white arrows**) cells. Tumor size was measured every 3 days; the **error bars** in (E) represent 95% CIs of the mean volume of eight tumors induced by OLC1-C1. **F**) Immunoblot analysis of OLC1 protein expression in MBE cell clones stably overexpressing OLC1 using the antibody in (A). Clone 4 (C4, also MBE-OLC1) was used in subsequent experiments because it had the highest level of OLC1 expression. **G**) In vitro growth of MBE-OLC1 and MBE-vector cells. **Error bars** represent 95% CIs from a representative experiment (counted from triplicate wells) of three independent ones. *MBE-OLC1 vs MBE-vector cells, $P = .005$; **$P < .001$. **H**) Colony formation assay of MBE-OLC1 and MBE-vector cells. Means and 95% CIs (**error bars**) are shown from three independent experiments performed in triplicate. *MBE-OLC1 vs MBE-vector cells, $P < .001$. **I**) Cell cycle analysis of MBE-OLC1 and MBE-vector cells. Cells (1×10^6) were stained with propidium iodide, and their DNA content was determined using flow cytometry. One representative experiment of three independent experiments is shown.

Discussion

In this report, we have demonstrated that *OLC1*, a gene that has not been previously characterized, was amplified and overexpressed in lung cancer. Forced overexpression of OLC1 caused malignant transformation of NIH3T3 cells both in vitro and in vivo. In the converse experiment, suppression of OLC1 expression in lung cancer cell lines induced apoptosis and growth arrest. OLC1 overexpression was associated with the smoking history of patients with lung cancer. We also provide evidence indicating that OLC1 overexpression may be involved in cigarette smoke–induced human lung carcinogenesis, especially at an early stage. Thus, *OLC1* is a candidate lung cancer oncogene whose expression may be regulated by exposure to cigarette smoke.

Over the past decade, much has been learned about the molecular alterations associated with lung cancer. However, the precise mechanisms underlying lung carcinogenesis remain unresolved. To identify differentially expressed genes in human lung SCC, we previously compared the expression profiles between cultured primary lung SCC tumor cells and bronchial epithelial cells from the same patient and between fresh lung SCC tissues and morphologically normal bronchial epithelia and constructed four cDNA libraries containing genes whose expression increased or decreased in human lung SCC using SSH (17,29). Fifty functionally unknown, novel genes were then selected from these SSH libraries, and the full-length open reading frames were assembled to study the potential involvement of these genes in lung carcinogenesis. Among these 50 genes, we found one gene whose expression was increased in human lung SCC and could induce NIH3T3 cell transformation with the increased foci formation. A series of in vitro and in vivo experiments were then carried out to further investigate the potential oncogenic effect of OLC1.

Our data demonstrated that NIH3T3 cells with exogenous OLC1 overexpression grew at an accelerated rate and gained the ability to undergo anchorage-independent growth. Furthermore, nude mouse xenograft studies showed that NIH3T3 cells

overexpressing OLC1, but not parental or empty vector control–transfected cells, produced fibrosarcomas. These results provide convincing evidence indicating that OLC1 is a candidate oncogene. We also examined the oncogenic role of OLC1 in MBE, an immortalized human bronchial epithelial cell line. The MBE cells with OLC1 overexpression showed an increased growth rate, colony formation, and cell cycle progression, but their growth in soft agar was similar to controls, and no tumors formed in nude mice inoculated with MBE-OLC1 cells (data not shown), indicating that OLC1 alone is not sufficient to transform bronchial epithelial cells.

We designed two siRNAs, both of which were able to successfully suppress OLC1 expression in the H520 and H1299 lung cancer cell lines. Cells in which OLC1 expression was silenced underwent obvious apoptosis in the absence of other apoptotic inducers, grew more slowly, and had reduced capacity for colony formation than control cells expressing OLC1. These OLC1 silencing results strongly support the hypothesis that OLC1 is oncogenic in human lung cancer cell lines.

We also showed that genomic amplification and overexpression of OLC1 occur in lung cancer cell lines and primary tumors. OLC1 gene amplification was observed in more than half of primary lung SCC

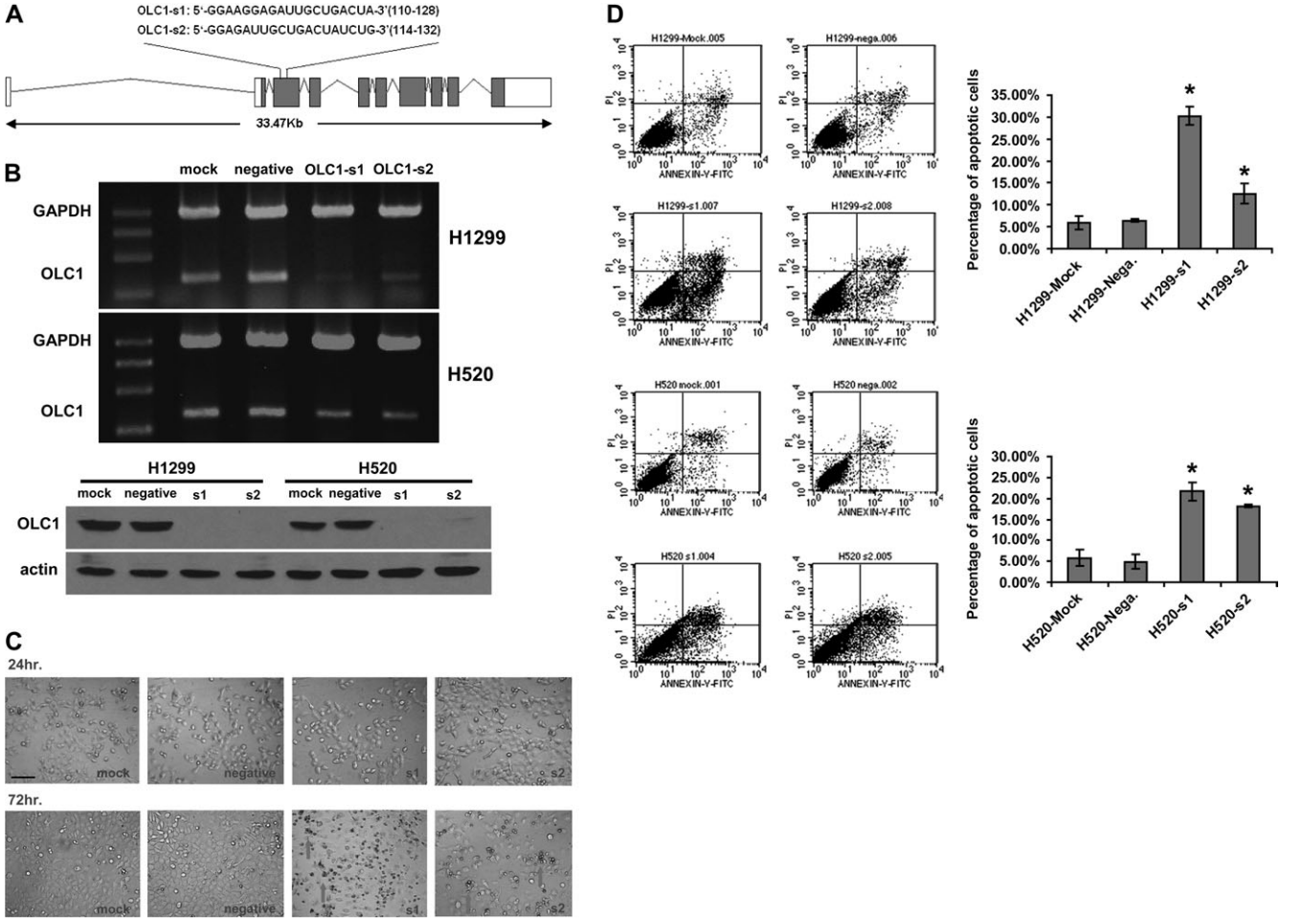

Figure 5. Effect of overexpressed in lung cancer 1 (OLC1) knockdown with small interfering RNAs (siRNAs) on lung cancer cell lines H1299 and H520. **A**) Schematic representation of two siRNAs (si1 and si2) against OLC1. The sense sequences are shown. **B**) OLC1 knockdown in H1299 and H520 cells. Top, reverse transcription polymerase chain reaction analysis performed at 48 h after siRNAs transfection. Bottom, OLC1 protein detected by immunoblotting using a polyclonal rabbit anti-OLC1 antibody 72 h after siRNAs transfection. Cells that were transfected with no siRNA (mock) or a scrambled siRNA (negative) were used as negative controls. **C**) Apoptosis in H1299 cells at 72 h after transfection with OLC1-s1 and -s2 by as observed by optical microscopy. **Arrows** indicate the shrinking apoptotic cells. Scale bar = 50 μm. **D**) Left, flow cytometric analysis of H1299 and H520 cells stained with annexin-V-fluoroisothiocyanate (FITC) and propidium iodide (PI). Cells were harvested 72 h after siRNA transfection. Right, the percentage of apoptotic cells represents the percentage of annexin-V–positive cells. Means from two independent experiments and 95% CIs (error bars) are shown. Error bars represent 95% CIs of the two experiments (*H1299 cells: s1 vs negative, $P = .002$; s1 vs mock, $P = .003$; s2 vs negative, $P = .035$; s2 vs mock, $P = .042$. H520 cells: s1 vs negative, $P = .007$; s1 vs mock, $P = .009$; s2 vs negative, $P = .004$; s2 vs mock, $P = .006$; Student two-sided *t* test). Similar results were obtained in two separate experiments. **E**) The tetrazolium salt 3-(4,5-dimethylthiazol-2-yl)-2,5-diphenyltetrazolium bromide proliferation assay of siRNA-transfected, mock, and negative H1299 and H520 cells. Error bars represent 95% CIs from one representative experiment with six replicates of three independent ones. *s1 or s2 vs negative, $P < .001$. **F**) Colony formation assay of siRNA-transfected, mock, and negative H1299 and H520 cells. Error bars represent 95% CIs from one representative experiment performed in triplicate of three independent ones (*H1299 cells: s1 vs negative control, $P < .001$; s1 vs mock control,

(continued)

Figure 5 (continued).

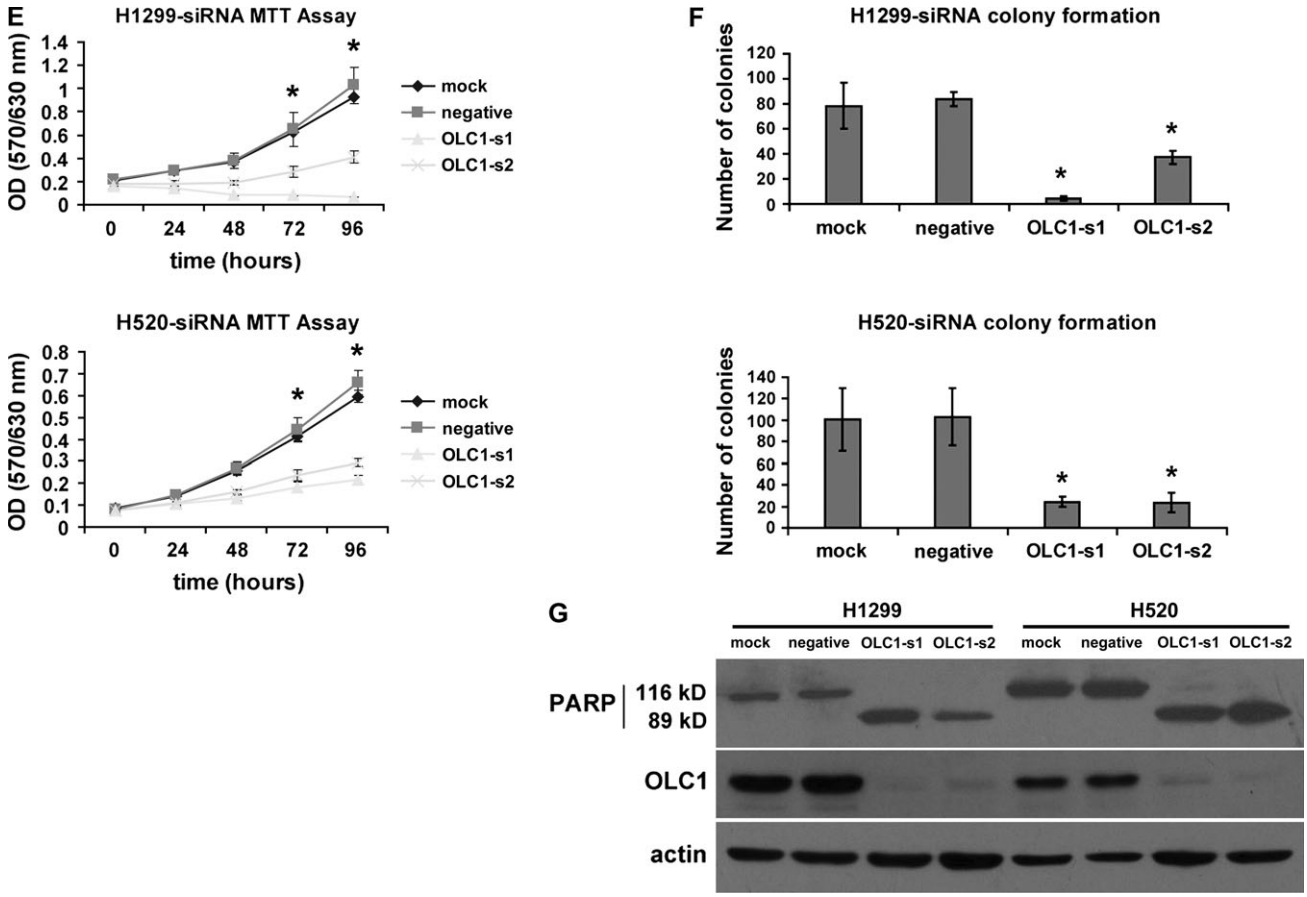

P = .001; s2 vs negative control, *P* < .001; s2 vs mock control, *P* = .014. H520 cells: s1 vs negative control, *P* = .005; s1 vs mock control, *P* = .007; s2 vs negative control, *P* = .005; s2 vs mock control, *P* = .008; Student two-sided *t* test). **G**) Immunoblot analysis of PARP cleavage using a rabbit polyclonal anti-PARP antibody 72 h after transfection. Cells were transfected with OLC1 siRNAs (OLC1-s1 and -s2), with no siRNA (mock), or with a scrambled siRNA (negative). Blots were probed with polyclonal rabbit anti-OLC1 and with anti–β-actin as a control for protein loading and transfer. One representative of three independent experiments is shown.

tested by FISH and real-time PCR. Results from IHC staining of tissue microarray containing more than 500 human lung cancer samples showed the overexpression of OLC1 in lung adenocarcinoma, SCLC, and SCC, the most common types of lung cancer. The evidence mentioned above strongly suggests that OLC1 is a candidate oncogene related to human lung cancer. During the preparation of this manuscript, another group reported a high-resolution genomic profile of human lung cancer with a 0.26-Mb amplicon at 16q22.2 (30). Although no oncogene had been previously identified in this region, it is where the OLC1 locus is found. The data here indicate that OLC1 overexpression in lung cancer is at least partially due to the amplification of OLC1 locus at 16q22.2.

Cigarette smoke is a well-known cause of human lung cancer and other upper aerodigestive tract tumors (13,31). Cigarette smoke condensate is a complex chemical mixture containing numerous carcinogens, mutagens, or tumor promoters that have been implicated in tumor initiation and promotion (32). The most potent carcinogenic agent contained in cigarette smoke condensate is NNK, which is formed by nitrosation of nicotine and has been thought to be the most important etiological factor in cigarette smoke–related cancers (33). We investigated the relationship between OLC1 overexpression and the smoking history of lung cancer patients. Results from IHC analyses clearly showed that OLC1 overexpression was related to the smoking history of lung cancer patients. In addition, our data demonstrate that OLC1 expression is elevated early in bronchial dysplasia/CIS, although no statistically significant differences were found with regard to tumor stage or grade. In vitro experiments further confirmed that cigarette smoke condensate treatment induced expression of OLC1 in all the cell types tested, and this effect of cigarette smoke condensate exposure was persistent and could be seen as late as 48 hours after the treatment. Our findings suggest that OLC1 overexpression may be involved in cigarette smoke–induced human lung carcinogenesis especially at early stage.

We have begun to explore the mechanism behind the oncogenic activity of OLC1. Using reporter assays for critical signaling pathways including NF-kappaB–, AP-1–, and nuclear factor of activated T-cells responsive promoters in HeLa cells, we found that OLC1 can activate an NF-kappaB reporter gene (see Supplementary Figure 5, available online). There is mounting evidence for the constitutive activation of the NF-kappaB pathway in numerous cancers, including lung cancer (34–36). Other recent studies have implicated NF-kappaB as a tumor promoter in inflammation-associated cancer

(37) and have shown that activation of NF-kappaB occurs early during neoplastic transformation of mammary cells (38), suggesting that NF-kappaB activation is an early event during carcinogenesis. Furthermore, cigarette smoke has been reported to activate NF-kappaB (39). Our preliminary results suggest that OLC1 may play a role in the IκBα/NF-kappaB activation involved in human lung carcinogenesis.

Studies are under way to explore the mechanism of OLC1-mediated oncogenesis. While we were cloning the 50 novel genes from the SSH library, another group carried out a large-scale screening of human genes that activate the MAPK signaling pathways (40). OLC1 was preliminarily listed in the Supplementary Data by this group as a MAPK activating gene (with the protein name putative MAPK activating protein PM28), but we failed to detect this activity in our studies of OLC1 in HEK293, 293T, and HeLa cells (see Supplementary Figure 6, available online).

Our study has several limitations. First, we have found only a preliminary association between the oncogenic role of OLC1 overexpression and cigarette smoke. More efforts should be made to illuminate the role of OLC1 in the cigarette smoke–mediated oncogenic process. We are currently developing a mouse model with normal or deficient OLC1 function to learn more about this process. Second, the detailed mechanisms of how overexpression of OLC1 induces tumorigenesis remain unknown, and further studies are needed to determine which oncogenic pathway OLC1 may be involved in.

Altogether, this study provides strong evidence supporting an important role for the novel gene OLC1 in the carcinogenesis of the human lung. The results indicate that cigarette smoke–induced overexpression of OLC1 may be involved at an early stage of human lung carcinogenesis.

References

1. Jemal A, Siegel R, Ward E, Murray T, Xu J, Thun MJ. Cancer statistics, 2007. *CA Cancer J Clin.* 2007;57(1):43–66.
2. Minna JD, Roth JA, Gazdar AF. Focus on lung cancer. *Cancer Cell.* 2002;1(1):49–52.
3. Hsu NY, Ho HC, Chow KC, et al. Overexpression of dihydrodiol dehydrogenase as a prognostic marker of non-small cell lung cancer. *Cancer Res.* 2001;61(6):2727–2731.
4. Hu Z, Lin D, Yuan J, et al. Overexpression of osteopontin is associated with more aggressive phenotypes in human non-small cell lung cancer. *Clin Cancer Res.* 2005;11(13):4646–4652.
5. Liao Z, Milas L. COX-2 and its inhibition as a molecular target in the prevention and treatment of lung cancer. *Expert Rev Anticancer Ther.* 2004;4(4):543–560.
6. Shintani Y, Higashiyama S, Ohta M, et al. Overexpression of ADAM9 in non-small cell lung cancer correlates with brain metastasis. *Cancer Res.* 2004;64(12):4190–4196.
7. Erez A, Perelman M, Hewitt SM, et al. Sil overexpression in lung cancer characterizes tumors with increased mitotic activity. *Oncogene.* 2004; 23(31):5371–5377.
8. Heighway J, Knapp T, Boyce L, et al. Expression profiling of primary non-small cell lung cancer for target identification. *Oncogene.* 2002; 21(50):7749–7763.
9. Sugita M, Geraci M, Gao B, et al. Combined use of oligonucleotide and tissue microarrays identifies cancer/testis antigens as biomarkers in lung carcinoma. *Cancer Res.* 2002;62(14):3971–3979.
10. Nacht M, Dracheva T, Gao Y, et al. Molecular characteristics of non-small cell lung cancer. *Proc Natl Acad Sci USA.* 2001;98(26): 15203–15208.
11. Bangur CS, Switzer A, Fan L, Marton MJ, Meyer MR, Wang T. Identification of genes over-expressed in small cell lung carcinoma using suppression subtractive hybridization and cDNA microarray expression analysis. *Oncogene.* 2002;21(23):3814–3825.
12. Greenlee RT, Hill-Harmon MB, Murray T, Thun M. Cancer statistics, 2001. *CA Cancer J Clin.* 2001;51(1):15–36.
13. Wingo PA, Ries LA, Giovino GA, et al. Annual report to the nation on the status of cancer, 1973–1996, with a special section on lung cancer and tobacco smoking. *J Natl Cancer Inst.* 1999;91(8):675–690.
14. Hoffmann D, Hoffmann I, El-Bayoumy K. The less harmful cigarette: a controversial issue. A tribute to Ernst L. Wynder. *Chem Res Toxicol.* 2001;14(7):767–790.
15. Mountain CF. The international system for staging lung cancer. *Semin Surg Oncol.* 2000;18(2):106–115.
16. Hirsch FR, Franklin WA, Gazdar AF, Bunn PA Jr. Early detection of lung cancer: clinical perspectives of recent advances in biology and radiology. *Clin Cancer Res.* 2001;7(1):5–22.
17. Sun W, Zhang K, Zhang X, et al. Identification of differentially expressed genes in human lung squamous cell carcinoma using suppression subtractive hybridization. *Cancer Lett.* 2004;212(1):83–93.
18. Lu YJ, Dong XY, Guo SP, Ke Y, Cheng SJ. Integration of SV40 at 12q23 in SV40-immortalized human bronchial epithelial cells. *Carcinogenesis.* 1996;17(9):2089–2091.
19. Neben K, Korshunov A, Benner A, et al. Microarray-based screening for molecular markers in medulloblastoma revealed STK15 as independent predictor for survival. *Cancer Res.* 2004;64(9):3103–3111.
20. Moch H, Sauter G, Gasser TC, et al. EGF-r gene copy number changes in renal cell carcinoma detected by fluorescence in situ hybridization. *J Pathol.* 1998;184(4):424–429.
21. Bertelsen BI, Steine SJ, Sandvei R, Molven A, Laerum OD. Molecular analysis of the PI3K-AKT pathway in uterine cervical neoplasia: frequent PIK3CA amplification and AKT phosphorylation. *Int J Cancer.* 2006; 118(8):1877–1883.
22. Kononen J, Bubendorf L, Kallioniemi A, et al. Tissue microarrays for high-throughput molecular profiling of tumor specimens. *Nat Med.* 1998;4(7):844–847.
23. Lu YJ, Guo SP, Tong T, et al. Establishment and characterization of a SV40T-transformed human bronchial epithelial cell line. *Lung Cancer.* 1998;19(1):15–24.
24. An Q, Pacyna-Gengelbach M, Schluns K, et al. Identification of differentially expressed genes in immortalized human bronchial epithelial cell line as a model for in vitro study of lung carcinogenesis. *Int J Cancer.* 2003;103(2):194–204.
25. Wang Y, Li X, Wang L, et al. An alternative form of paraptosis-like cell death, triggered by TAJ/TROY and enhanced by PDCD5 overexpression. *J Cell Sci.* 2004;117(pt 8):1525–1532.
26. Cerami C, Founds H, Nicholl I, et al. Tobacco smoke is a source of toxic reactive glycation products. *Proc Natl Acad Sci USA.* 1997;94(25):13915–13920.
27. Guo Z, Linn JF, Wu G, et al. CDC91L1 (PIG-U) is a newly discovered oncogene in human bladder cancer. *Nat Med.* 2004;10(4):374–381.
28. Liang KY, Zeger SL. Longitudinal data analysis using generalized linear models. *Biometrika.* 1986;73(1):13–22.
29. Liu Y, Sun W, Zhang K, et al. Identification of genes differentially expressed in human primary lung squamous cell carcinoma. *Lung Cancer.* 2007;56(3):307–317.
30. Tonon G, Wong KK, Maulik G, et al. High-resolution genomic profiles of human lung cancer. *Proc Natl Acad Sci USA.* 2005;102(27): 9625–9630.
31. Do KA, Johnson MM, Lee JJ, et al. Longitudinal study of smoking patterns in relation to the development of smoking-related secondary primary tumors in patients with upper aerodigestive tract malignancies. *Cancer.* 2004;101(12):2837–2842.
32. Smith CJ, Livingston SD, Doolittle DJ. An international literature survey of "IARC Group I carcinogens" reported in mainstream cigarette smoke. *Food Chem Toxicol.* 1997;35(10–11):1107–1130.
33. Hecht SS. Tobacco smoke carcinogens and lung cancer. *J Natl Cancer Inst.* 1999;91(14):1194–1210.

34. Fujioka S, Sclabas GM, Schmidt C, et al. Inhibition of constitutive NF-kappa B activity by I kappa B alpha M suppresses tumorigenesis. *Oncogene*. 2003;22(9):1365–1370.
35. Javelaud D, Poupon MF, Wietzerbin J, Besancon F. Inhibition of constitutive NF-kappa B activity suppresses tumorigenicity of Ewing sarcoma EW7 cells. *Int J Cancer*. 2002;98(2):193–198.
36. Biswas DK, Shi Q, Baily S, et al. NF-kappa B activation in human breast cancer specimens and its role in cell proliferation and apoptosis. *Proc Natl Acad Sci U S A*. 2004;101(27):10137–10142.
37. Pikarsky E, Porat RM, Stein I, et al. NF-kappaB functions as a tumour promoter in inflammation-associated cancer. *Nature*. 2004;431(7007):461–466.
38. Kim DW, Sovak MA, Zanieski G, et al. Activation of NF-kappaB/Rel occurs early during neoplastic transformation of mammary cells. *Carcinogenesis*. 2000;21(5):871–879.
39. Anto RJ, Mukhopadhyay A, Shishodia S, Gairola CG, Aggarwal BB. Cigarette smoke condensate activates nuclear transcription factor-kappaB through phosphorylation and degradation of IkappaB(alpha): correlation with induction of cyclooxygenase-2. *Carcinogenesis*. 2002;23(9):1511–1518.
40. Matsuda A, Suzuki Y, Honda G, et al. Large-scale identification and characterization of human genes that activate NF-kappaB and MAPK signaling pathways. *Oncogene*. 2003;22(21):3307–3318.
41. Thompson JD, Gibson TJ, Plewniak F, Jeanmougin F, Higgins DG. The CLUSTAL_X windows interface: flexible strategies for multiple sequence alignment aided by quality analysis tools. *Nucleic Acids Res*. 1997;25(24):4876–4882.

Funding

This work was supported by grants of the State Key Program of Basic Research (2004CB518707 to S.C. and Y.G.), the National High Technology Research and Development Program of China (2002BA711A01 to D.M., 2002BA711A06 to Y.G.), the National Natural Science Foundation of China (30572095 to Y.G.), and Beijing Municipal Key Project (D0905001040731 to Y.G. and S.C.). The sponsors had no role in the study design, the analysis and interpretation of the data, the preparation of the manuscript, or the decision to submit the manuscript for publication.

Notes

J. Yuan, J. Ma, and H. Zheng contributed equally to this work.

We thank Dr Jin Jen and Dr Li Mao for their stimulating discussions and valuable comments of this manuscript, Dr Chunxiao Wu for his help with some assays, and Dr Yilong Wang for his assistance with statistical analysis.

Manuscript received January 31, 2008; revised August 25, 2008; accepted September 19, 2008.